

9

Wind

Owing to the development of motor transport, it is possible to study in the further interiors of the great deserts the free interplay of wind and sand, uncomplicated by the effects of moisture, vegetation, or of fauna, and to observe the results of that interplay extended over great periods of time.

Here, instead of finding chaos and disorder, the observer never fails to be amazed at a simplicity of form, an exactitude of repetition and a geometric order unknown in nature on a scale larger than that of crystalline structure.

R. A. Bagnold (1941)

Ralph Bagnold (1896–1990) founded our modern understanding of the interaction between wind and sand and how that interaction produces dune-covered landscapes in the Earth's great deserts. He lived to see spacecraft images of the sand seas on Mars and contributed to our understanding of how universally important wind-driven (eolian) processes are. He would have been delighted to know about the extensive dune fields of tarry sand on Titan.

Bagnold was a professional soldier and the descendent of a long line of professional soldiers (Bagnold, 1990). After an engineering education at Cambridge, he was posted to Egypt in 1926 and then to other locations in North Africa where he became fascinated by the landscape and decided to devote himself to the study of that region's most abundant commodity – sand. In addition to unprecedented trips deep into the deserts of Sudan and Libya, he built a wind tunnel out of plywood at Imperial College, London, to further his understanding of the interaction of wind and sand. His classic book was published in 1941.

One of his major insights about this process is best stated, once again, in his own words,

After much desert travel, extending over many years, during which sandstorms of varying intensity were frequently encountered, I became convinced that the movement of sand (as opposed to that of dust) is a purely surface effect, taking place only within a metre of the ground.

(Bagnold, 1941)

Bagnold used this insight to justify his reliance on wind-tunnel observations. Much more elaborate and expensive wind tunnels than Bagnold's are now used to simulate sand

transport under both Martian and Venusian conditions. Modern research has also moved outdoors and focuses on the interaction of dunes with both local winds and the planetary boundary layer, but many mysteries still remain and new insights are still needed to fully understand the dynamics of how the wind interacts with granular materials on planetary surfaces.

Following Bagnold's lead, this chapter is more mathematical than any other in this book. Bagnold quite appropriately put the word "physics" into the title of his book and insofar as physics requires the language of mathematics, the study of eolian processes has, since Bagnold, always relied heavily on that mode of expression. As we shall see, however, the mathematics required does not go much beyond algebra: When really intricate analyses are required, such as the structure of turbulent boundary layers, Bagnold himself resorted to empirical models, and we shall do the same.

Eolian processes are concerned with a gas, the atmosphere, and granular solids. A discussion of interactions between the atmosphere and a liquid is reserved for the next chapter.

9.1 Sand vs. dust

The mechanical distinction between sand and dust is simple: Dust is easily suspended in the atmosphere while sand, under a moderately strong wind, hops along the surface. However, quantifying this distinction for a wide variety of solid particles in different planetary atmospheres requires some careful discussion, as does the meaning of a "moderately strong" wind. The first step in this discussion is to understand how solid particles fall through air.

9.1.1 Terminal velocity

Students in freshman physics courses are encouraged to ignore atmospheric drag while they learn Galileo's formulas for falling bodies. However, every skydiver's life depends on the fact that these formulas do not accurately describe his or her descent toward the surface of the Earth. A human body falling out of an airplane rapidly accelerates, initially following Galileo's rules, but within about 15 s achieves a constant velocity known as the terminal velocity. This is about 200 km/hour for a human body in Earth's atmosphere. If this were the end of the story, our skydiver's arrival at the Earth's surface would still be very uncomfortable and skydiving would not be a popular sport. However, the terminal velocity is a balance between the weight of a falling body and the drag force exerted on it by the passing air. This drag force can be greatly enhanced by increasing the area of the falling body – which is what parachutes are intended to do.

Quantitative analysis of the terminal velocity requires some simplifications. In the best tradition of physics, we now consider a spherical sand grain (which is not such a bad approximation as either the traditional spherical cow or a spherical skydiver!). The force accelerating the grain toward the Earth is its weight, w , equal to its mass m times the acceleration of gravity g . Expressing this in terms of the grain diameter d and density σ , the driving force is:

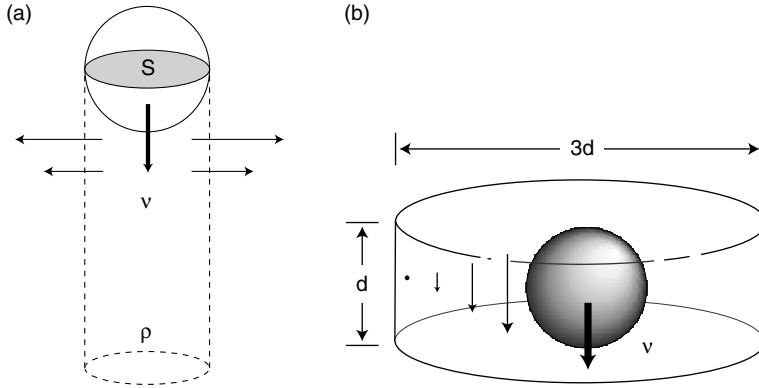


Figure 9.1 Terminal velocity force balance for (a) turbulent flow, where the weight of the grain is balanced against the momentum change of air displaced by the motion of the grain and (b) laminar flow, where the weight of the grain is balanced by viscous drag forces, here approximated as being localized in a cylinder with a diameter three times larger than the grain diameter d . In this case the velocity of the air equals the velocity of the grain at the grain surface but drops to zero (approximately) at the surface of the cylinder.

$$w = \frac{\pi}{6} d^3 (\sigma - \rho) g. \quad (9.1)$$

In this equation ρ is the density of the air, so that the weight is really the immersed weight, which takes account of the buoyancy of the fluid that surrounds the grain. This correction may seem to be negligible for quartz sand (density about 2650 kg/m^3) in the Earth's atmosphere (density 1.2 kg/m^3); however, we shall see that the equations that we derive for sand and air apply almost without alteration for sand and water or any other liquid, where the buoyancy correction may be substantial, so we will retain this distinction in the following analysis.

The drag force is more complex and requires our first empirical injection. Simple consideration of the momentum of the air deflected by the particle (Figure 9.1a) suggests that it should depend on the projected area of the falling grain, $\pi d^2/4$, the density of the air ρ and the square of the relative velocity v between the grain and the air. However, the exact drag force depends on the shape of the grain and its velocity in a more complicated way, so this complexity is absorbed into a mostly empirical constant called the drag coefficient C_D , defined so that the drag force F_D comes out as:

$$F_D = C_D \frac{\pi \rho d^2 v^2}{4}. \quad (9.2)$$

Over a wide range of velocities, $C_D \approx 0.4$ for a sphere.

Equating the weight (9.1) and drag force (9.2) and solving for the velocity yields an expression for the terminal velocity:

$$v = \sqrt{\frac{4(\sigma - \rho)dg}{3C_D\rho}}. \quad (9.3)$$

As one might expect, objects fall faster if they are denser, bigger, or the acceleration of gravity is higher. They fall more slowly if the air density or drag coefficient is higher.

Equation (9.3) does not hold for all grain sizes. In particular, it may give an extremely poor estimate of the terminal velocity for small particles unless the drag coefficient is changed rather substantially. This equation holds best in what is called the turbulent regime, where drag forces are created by the deflection of the air stream. The vigilant reader may also be surprised that there is no dependence on the viscosity of the air in this equation. Viscosity is important only for very small or slow particles. The dividing line between turbulent flow and the low-velocity laminar flow regime is determined by the Reynolds number Re , which is the ratio between inertial and viscous forces,

$$Re = \frac{\rho vd}{\eta}. \quad (9.4)$$

When the Reynolds number is low, inertial forces are small compared to viscous forces, and viscosity, not the deflection of the air stream, determines the drag force. George G. Stokes (1819–1903) first analyzed the full equations for viscous drag in 1851 and the terminal velocity for a sphere is now called Stokes' law. The full derivation is complex and not very edifying, so I instead present an approximate derivation that captures the essence of the equation.

Suppose that our small falling sphere is surrounded by a cylindrical can of diameter $3d$ and height d (Figure 9.1b). We suppose that the velocity of the air is zero on the surface of the can, but equals the velocity of the sphere at the sphere's surface. This is not really true: The air velocity falls off more gradually with distance away from the sphere, but most of its decline is close to the sphere, so our rigid can is a good first approximation. The air between the sphere and the can is, thus, sheared with a strain rate $\dot{\epsilon} \approx v/2d$. Remembering that the definition of viscosity, Equation (3.12), is $\sigma_s = 2\eta\dot{\epsilon}$, where σ_s is the shear stress, we obtain the drag force by multiplying the shear stress times the surface area of the vertical sides of the can, $3\pi d^2$. Equating this drag force to the weight of the grain, (9.1), and solving for the velocity, we obtain the terminal velocity of a small particle for which $Re \ll 1$,

$$v = \frac{1}{18} \frac{(\sigma - \rho)d^2g}{\eta} \quad (9.5)$$

which happens to be exactly Stokes' law, thanks to a clever choice of the dimensions of our cylindrical can. Another way to achieve this result is to note that at low Reynolds number the drag coefficient is given by $C_D = 24/Re$, which upon substitution into (9.3) yields Stokes' law.

The most notable features of Stokes' law are its inverse dependence on gas viscosity and its dependence on the square of the particle diameter. This means that the terminal velocity

of very small particles is very low. Anyone who has wondered why the clouds, composed of tiny water droplets with mean radii of about $10\ \mu\text{m}$, do not fall out of the sky can answer this question for themselves by evaluating Equation (9.5) for a cloud droplet.

Stokes' law is valid for Reynolds numbers less than about 10, while the turbulent drag equation holds for Reynolds numbers between about 10^3 and 10^5 . Between these regimes empirical expressions for the drag coefficient must be used to compute the terminal velocity.

Evaluation of the terminal velocities of small particles in the atmospheres of different planets requires the viscosity of the gas. This can be derived from experiment or looked up in a table. However, it is useful to note a few results on gas viscosity from the kinetic theory of gases. Most importantly, the viscosity of a gas is nearly independent of pressure. Thus, whether we are dealing with air at the Earth's surface or air in the stratosphere, the viscosity η is the same (at the same temperature). J. C. Maxwell first deduced this fact from his kinetic theory of gases and, at first, he could not believe it: Checking this prediction was the motivation for his 1867 experiments that also led him to invent the concept of a Maxwell solid (Section 3.4.3). This surprising behavior comes about because the viscosity of a gas is the consequence of the exchange of momentum between layers of gas moving relative to one another. As pressure decreases there are fewer gas molecules to exchange momentum, but their mean free path increases at the same time, so the exchange takes place between layers of greater relative velocity. The two factors cancel one another and the resulting viscosity is independent of pressure. Maxwell also predicted that the viscosity of a gas depends on the square root of the temperature. This prediction is less accurate: Measurements show that in most gases the viscosity depends more strongly upon temperature. Subsequent research connects the temperature dependence of viscosity to the forces between molecules, so this dependence must usually be determined empirically.

Table 9.1 lists the terminal velocities of small spheres based on Stokes' law for silicate grains near the surface of Earth, Mars, and Venus, along with velocities for tarry organic grains on Titan. It is clear that as particle size decreases the terminal velocity decreases rapidly as well. For a given size particle the terminal velocities are surprisingly similar despite the wide differences between the various bodies. The major determinant of terminal velocity is grain size, not which planet it falls on. Note that for grains larger than $100\ \mu\text{m}$ Stokes' law underestimates the terminal velocity and a more accurate expression for the drag coefficient must be used.

9.1.2 Suspension of small particles

The terminal velocity alone is not enough to estimate whether a particle will be suspended or sink to the surface. In a quiet atmosphere, or if the wind flow was purely laminar, particles of all sizes would eventually settle to the surface. However, the atmosphere of a planet is almost never completely quiet or laminar. Winds are ultimately due to the spherical shapes of planets and the fact that solar radiation is not uniformly distributed over their surfaces. Because of inequalities of heating, currents arise in the atmosphere.

Table 9.1 *Terminal velocities of small particles*

Body	Particle composition, density (kg/m ³)	Gas viscosity (10 ⁻⁶ Pa-s)	100 μm grain diameter (m/s)	30 μm grain diameter (m/s)	10 μm grain diameter (m/s)
Venus	Silicate, 2700	33.0	0.40	0.036	0.0040
Earth	Silicate, 2700	17.1	0.88	0.079	0.0088
Mars	Silicate, 2700	10.6	0.55	0.05	0.0055
Titan	Organic tar, 1500	6.3	0.18	0.016	0.0018

The flow of all known planetary atmospheres is turbulent. The air does not travel smoothly from one point to another. Instead, instabilities in the flow develop that lead to wide fluctuations of the instantaneous velocity about the mean. Turbulent flow develops when the Reynolds number, Equation (9.4), is large, and at the scale of planetary atmospheres it is invariably very large. Turbulence is a broad and complex subject, which is treated in many specialized books devoted to that topic (a good introduction is Tennekes and Lumley, 1972). At the moment what it means to us is that the motion of the atmosphere can be divided into two components: an average wind speed that remains constant for long periods of time, and a fluctuating component that varies widely over short timescales.

The full story of how particles can be suspended in fluids is surprisingly complex, relying on the phenomenon of “bursting” in turbulent fluids to inject momentum from the surface boundary layer into the body of the moving fluid. For the purposes of this book we will bypass this difficult topic and apply Bagnold’s rule of thumb, which states that the average velocity of turbulent eddies in a flow of air is equal to 1/5 of the mean velocity. Thus, for a wind velocity of a few meters per second, the turbulence velocity is about 0.5 m/s, so that the dividing line between sand and dust is about 100 μm on the terrestrial planets. It may be somewhat larger on Titan.

9.2 Motion of sand-sized grains

Grains too large to be suspended in the atmosphere may, nevertheless, be quite mobile on the surface under the influence of the wind. The hopping motion of sand grains along a river bed was first described by G. K. Gilbert (1914), who observed the process while studying the ability of water to transport river sediments. Gilbert called this motion “saltation” following McGee (1908), who took the term from the Latin word *saltus*, “leap.” Bagnold accepted this term and applied it to the much larger hops that sand grains executed in his wind tunnel.

Modern studies of eolian transport distinguish four modes of wind-driven particle motion. Suspended material is carried aloft by turbulent winds. Saltating grains hop from the surface, travel for some distance (the “saltation length”) with the air stream, and then reimpact

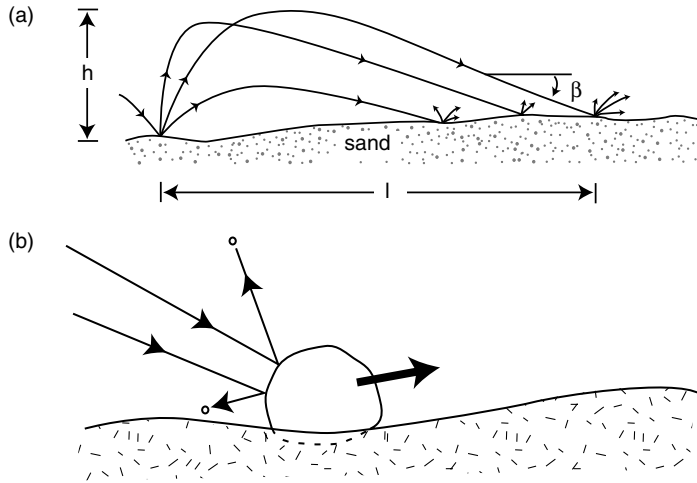


Figure 9.2 (a) Trajectories of saltating sand grains start out steeply as the grain is ejected from the surface. Near the apex of their hops, saltating grains attain a constant velocity and then follow a sloping (at angle β) linear trajectory as they fall back to the surface at terminal velocity, where they may initiate hops of other grains. The hop height is h and the length of each saltation hop is l . (b) Impact creep occurs as objects too large to saltate are struck by saltating grains. The momentum imparted by each impact pushes the larger grain downwind along the surface.

the surface (Figure 9.2a). Sand grains splashed out of the surface when saltating grains touch down either initiate new hops of their own or slither downwind in a snakelike motion called “reptation.” Larger sand grains and pebbles too large to hop may still move downwind under the impact of saltating grains, a motion called “impact creep” (Figure 9.2b) that includes rolling along the surface.

9.2.1 Initiation of motion

All the modes of wind transport, except perhaps suspension, require sand grains to be in saltating motion. The problem of how this motion starts from an initial state in which the wind begins to blow over a motionless sand bed has turned out to be both complex and revealing. Before we can begin a full discussion of this process, we need a better understanding of how the wind interacts with the surface.

Wind near the surface. The first real understanding of how a moving fluid interacts with a surface grew out of the studies of German aerodynamicist Ludwig Prandtl (1875–1953). Prandtl spent most of his career at Göttingen University. His major claim to fame is the concept of the boundary layer, a zone of sharply increasing velocity at the interface between a moving fluid and a solid surface. When Bagnold needed more information about how sand grains could begin moving away from a sandy surface, he corresponded with Prandtl and incorporated many of Prandtl’s ideas into his work.

The first important concept is the friction velocity v_* . The actual velocity varies with height above the surface in a complicated way that we will explore in a moment, but the

friction velocity is meant to express the overall effect of the wind on the surface by a single number that is independent of height. The friction velocity is defined in terms of the shear stress τ that the wind exerts on the surface. You could imagine measuring this wind shear on an ice-covered lake by cutting a small raft of ice free of the cover, then measuring the force with which the raft is pushed downwind while the wind is blowing. The shear stress τ is then the force divided by the area of the raft. The shear stress does not depend on the details of the velocity distribution above the surface – it is a single overall measure of the surface force of the wind. The friction velocity is then *defined* in terms of the shear stress as:

$$v_* \equiv \sqrt{\frac{\tau}{\rho}}. \quad (9.6)$$

The friction velocity is a central concept in theories of wind transport because it is directly related to the force the wind exerts on the surface (and vice versa). However, it is not often practical to measure the shear stress directly. Fortunately, the friction velocity has a simple, almost universal, relationship to the velocity above the surface. The following formula is partly empirical and partly can be derived from Prandtl's mixing length theory of turbulence. It relates the mean wind velocity to height z through the friction velocity and a factor known as "roughness," z_0 :

$$v(z) = 5.75 v_* \log\left(\frac{z}{z_0}\right). \quad (9.7)$$

The roughness factor is somewhat empirical. It is proportional to the grain size in the surface and approximately equal to 1/30 of the grain size when the grains are tightly packed. For Earth it is typically about 0.2–0.3 mm and it is usually assumed to be about the same on Mars. The roughness of many different surface types has been calculated by measuring wind velocities at different heights above the ground. Given tables of roughness it is possible to convert a wind speed measurement at a single height into a prediction of its value at any other height, as well as to obtain the friction velocity.

Equation (9.7) describes the velocity dependence some distance above the surface. However, it cannot hold down to scales comparable to the roughness because the flow is broken up by the irregularities of the surface. If the roughness is small, another distance scale becomes important, one controlled by the molecular viscosity of the gas. A layer in which turbulence is suppressed then develops next to the surface. Called the viscous sublayer, the thickness of this zone (also empirically determined) is:

$$\delta \approx 5 \frac{\eta}{\rho v_*}. \quad (9.8)$$

The numerical factor is empirical, while the dimensional ratio is derived from turbulence theory (Tennekes and Lumley, 1972). Within the viscous sublayer the velocity falls linearly to zero at the surface. The overall dependence of wind velocity on height above the surface is illustrated in Figure 9.3.

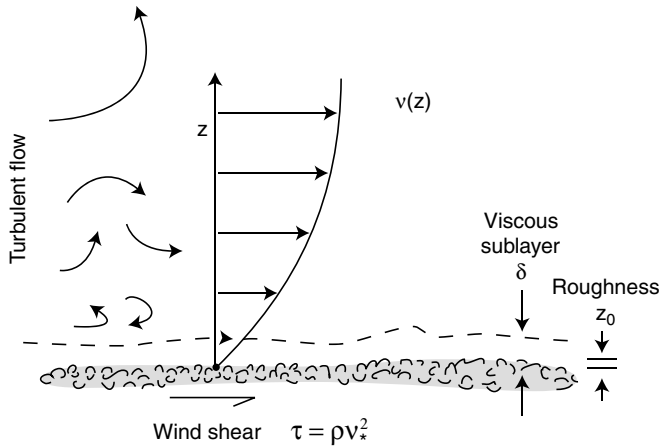


Figure 9.3 Mean velocity profile of wind over a sand surface. Turbulent eddies produce a logarithmic profile of mean velocity above the surface. Very close to the surface, viscous forces dominate and the fluid velocity falls linearly to zero through a viscous boundary layer of depth δ . The surface roughness is characterized by the parameter z_0 , while the average wind drag on the surface is related to the friction velocity v_* .

The fluid threshold. When the wind blows over a sand surface where no grains are yet in motion, it has to begin by plucking individual grains out of the surface before the wind stream can accelerate them. Supposing that the grains protrude above the viscous sublayer, each grain experiences a downwind force that is given by the shear stress τ times its projected surface area, $\pi d^2/4$. This drag force is resisted by the weight of the grain (which is decreased by the lift provided by the deflected wind stream), Figure 9.4 and Equation (9.1). Whether the wind actually succeeds in plucking an individual grain out of the surface depends on the geometry of its contacts and the way it deflects the wind, so an exact formula for a real surface is not possible. However, the drag force must equal the weight times some factor of order 1. Calling this factor A^2 and replacing τ by its definition in terms of the friction velocity (9.6), we solve the resulting equation for the threshold friction velocity at which motion just begins:

$$v_{*t} = A \sqrt{\left(\frac{\sigma - \rho}{\rho}\right) g d}. \tag{9.9}$$

The threshold velocity is proportional to the square root of the particle size, so this expression predicts, not surprisingly, that larger grains are more difficult for the wind to pick up than smaller ones.

Something new happens, however, when we consider very small grains. When the size of the grains becomes smaller than the thickness of the viscous sublayer, Equation (9.8), the wind drag is spread over a large number of particles: it is not localized on a single grain. The grains, thus, become more difficult to pull out of the surface and the wind velocity

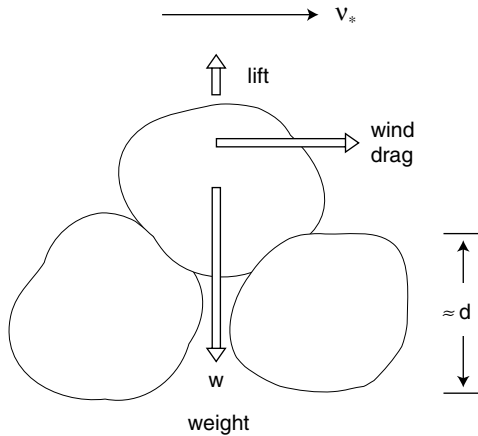


Figure 9.4 Forces acting on a grain resting on a surface of other grains of similar size. Each grain is subject to a drag force from the surface wind, possible lift forces from the deflected wind, friction between grains, and gravity holding it down onto the surface. Drag and lift forces must exceed friction and gravity before a grain begins to move.

must be higher than Equation (9.9) predicts before motion can start. There is a similar extra resistance if the grains stick together by cohesive forces, such as electrostatic or van der Waals forces, which are important for very small grains.

A full analysis of the effects of sublayer resistance is not presently possible. Instead, we must rely on empirical measurements of threshold velocities. Bagnold faced this problem and observed that, although the factor A in Equation (9.9) is roughly equal to 0.1 for large sand grains, it increases rapidly with decreasing particle size below some threshold (Figure 9.5). He found that A is a function of a dimensionless parameter that he called the “friction Reynolds number” Re_* . This Reynolds number is defined like the usual one, Equation (9.4), except that the friction velocity replaces the fluid velocity. For a friction Reynolds number less than about 3.5 the threshold velocity shoots up steeply (Figure 9.6) and appears to depend on Re_* to a large negative power. The appearance of the friction Reynolds number makes a lot of sense in this context because comparison of the definition of Re_* with the thickness of the viscous sublayer indicates that $d/\delta = 5/Re_*$. All this limit says is that the threshold velocity shoots up when the particle size is equal to about 0.7δ .

The approximate dependence of the threshold velocity on grain size can be derived from the dependence of A on Re_* , even though the power n is not well known. If A is a function of $1/Re_*^n$, then it also depends on $1/v_{*t}^n d^n$ (neglecting other terms in the relationship, which are not important for this argument). Inserting this dependence into Equation (9.9) and solving for v_{*t} , we find that it must depend on grain size d to the power $(1/2-n)/(n+1)$. But for large n , this ratio approaches -1 , so that we can say that for small grain sizes, v_{*t} depends approximately on $1/d$. Clearly, as d decreases the threshold velocity rises. But for $Re_* \gg 3.5$ we know that $A = 0.1$, and v_{*t} is proportional to \sqrt{d} . The threshold velocity, thus, rises rapidly for both large and small particle sizes (Figure 9.6). So we must conclude

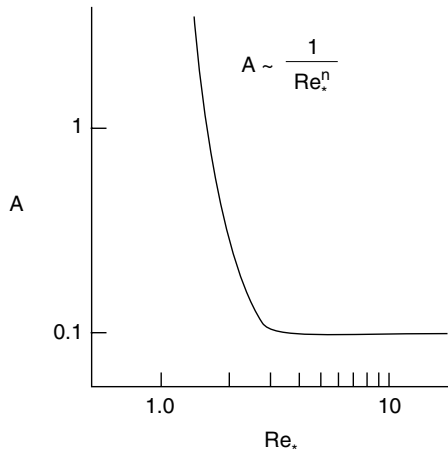


Figure 9.5 Dependence of the friction coefficient A in Equation (9.9) on the friction Reynolds number Re_* . The coefficient is nearly constant with a value 0.1 until Re_* falls below a critical limit, below which it rises rapidly.

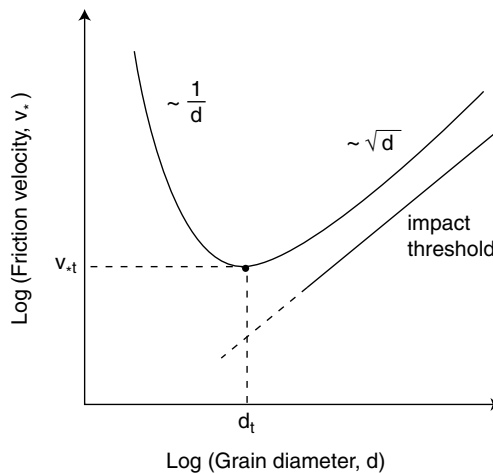


Figure 9.6 The threshold velocity for sand motion over an initially static sand bed has a pronounced minimum as a function of grain size. Small grains are buried in the viscous boundary layer and so are difficult to individually pluck out of the surface, while large grains are too heavy to move easily. This results in a unique size that is most easily entrained by the wind, at a corresponding minimum wind velocity. The threshold is much lower (the impact threshold) when sand grains are already in motion. Inspired by Bagnold (1941, Figure 28).

that there is a minimum for some special grain size that lies between the large particle and small particle limits.

The existence of a minimum in the threshold velocity curve has profound implications for wind- (and water-) transported material on any planet. It means that there is a special grain size, unique to that planet (and process, wind or water), which is most easily moved

and which, therefore, characterizes all the deposits emplaced by that process. The diameters of wind-transported sand grains on Earth nearly all lie within a narrow range, 0.1 to 0.3 mm (Ahlbrandt, 1979). This reflects the selection of the most easily moved grains by winds whose strength may vary, but the size of the grains that move first and most often is always close to the minimum of the curve. Water-deposited sands on beaches and in rivers show a wider variety of sizes owing to their frequently complex histories. In principle, we should be able to distinguish wind-blown sands from water-deposited sands because of the difference in threshold diameter. In practice this is not usually possible for a variety of reasons, and other criteria such as shape or surface texture are now used (Siever, 1988).

The actual value of the threshold diameter and velocity can be estimated from the information already presented by setting $A = 0.1$ in Equation (9.9) and using Bagnold's observation that Re_* at the threshold equals 3.5 to determine v_{*t} . The resulting equations can be solved for the grain diameter at the threshold, with the result:

$$d_t = 10.7 \left[\frac{\eta^2}{\rho(\sigma - \rho)g} \right]^{1/3}. \quad (9.10)$$

The corresponding threshold velocity is most easily derived from the Reynolds number at the threshold and the above equation:

$$v_{*t} = 3.5 \frac{\eta}{\rho d_t}. \quad (9.11)$$

These equations only approximately determine the minimum, which is rather broad in practice, so the precise values have to be taken with some skepticism, but using the same formulas to compare the onset of wind transport on different bodies is revealing. Table 9.2 lists the threshold grain diameters and velocities for the wind surface conditions on those Solar System bodies with substantial atmospheres. Where applicable, we also list the initiation conditions for flow in liquids that may be present on the surfaces of these bodies.

In order of ease of transport by wind, we see that the progression is Venus, Titan, Earth, and Mars. The threshold speeds are especially high on Mars, a fact that presents some problems that will be discussed separately. Wind speeds exceeding the threshold have been directly observed on Venus, Earth, and Titan. Dune fields have been observed on all three bodies, consistent with the predictions. The fact that extensive dune fields are also observed on Mars calls for special consideration.

The threshold grain size increases in the same progression, from very fine on Venus to very coarse on Mars. The predicted size for Earth is in fair agreement with the sizes commonly observed for dune sands.

Liquid is much denser than gas and so it can move particles with greater ease than the wind. The threshold equations also predict that it can move coarser particles (Mars, again, is an exception).

Grains at the threshold size are not the only ones that can be moved. The minimum in the curve is, observationally, rather broad (Greeley and Iversen, 1985) and winds higher than the minimum often occur, so that a range of grain sizes is usually transported. Greeley

Table 9.2 *Threshold grain diameters and fluid velocities*

Body	Medium	Viscosity (10^{-6} Pa-s)	Threshold diameter (μm)	Threshold friction velocity (m/s)	Fluid velocity at 1 m ^a (m/s)
Venus	Quartz in CO ₂	33.0	94	0.018	0.37
Earth	Quartz in air	17.1	220	0.21	4.50
Earth	Quartz in water	1540	560	0.01	0.21
Mars	Quartz in CO ₂	10.6	1100	3.3	69.
Mars	Quartz in water	1540	770	0.007	0.15
Titan	Tar in N ₂	6.30	160	0.025	0.53
Titan	Tar in liquid methane	184	410	0.004	0.080
Titan	Ice in liquid methane	184	530	0.003	0.062

^a Assuming roughness $z_0 = 2 \times 10^{-4}$ m.

and Iversen, in their book, tend to downplay the role of the viscous sublayer in raising the fluid threshold for small particles and instead emphasize cohesive forces between the grains. Electrostatic forces, however, tend to have the opposite effect and strong electric fields in the saltating layer may actually lift small particles off the bed (Kok and Renno, 2009b). It is clear that, even after 70 yr of study, there is still more to be learned about the fluid threshold.

The impact threshold. When sand grains are already in motion, they impact the surface at the end of their saltation hops and often knock other grains into the air. In this case the wind does not have to blow as fast as it does when the surface is quiescent. It is, thus, easier to keep grains in motion, once they have begun moving, than it is to initiate their first motion. This is an example of history-dependence of a process, or hysteresis. Of course, if the wind speed drops too low all of the sand grains fall back onto the surface and the process stops, but there is a range of wind speeds between the threshold speed and this stopping speed where sand motion is possible. The minimum velocity to keep grains in motion is known as the impact threshold and is indicated on Figure 9.6 by the line labeled “impact threshold.”

Bagnold’s experiments suggested to him that the impact threshold is given by Equation (9.9), with A equal to 0.08, rather than 0.1 at the fluid threshold (Figure 9.6). This estimate of Bagnold’s has been supported by subsequent research, which places A between 0.08 and 0.085 at the fluid threshold (Kok and Renno, 2009a). Naturally there is no upturn reflecting the viscous sublayer, but the decrease in surface velocity due to the grains already in motion may be significant. Saltating grains in water do not approach the surface with as high a velocity as those in air and so impacts may not be a strong factor in this case. However, other phenomena, such as turbulent bursting, may play a role in making the curve different for sediment in motion versus that for clean fluid just initiating motion.

A recent and important contribution to this topic (Kok, 2010) suggests that the impact threshold may be far more important for sand transport on Mars than it is on Earth. This

is a consequence of the very high speeds needed to reach the fluid threshold in Mars' thin atmosphere (Table 9.2). Once in motion, grains driven by high winds eject an exceptionally large number of grains from the surface. Taking account of the role of occasional gusts of high speed in initiating grain motion, it seems that winds with speeds ten times slower than the nominal fluid threshold prediction may, nevertheless, be effective in transporting sand and explain the many observations of eolian features on Mars, despite the few instances of winds high enough to reach the fluid threshold.

9.2.2 Transport by the wind

Once a few grains begin to move, the saltating grains knock others out of the surface, which themselves knock still other grains free, until the entire sand surface becomes covered by a low carpet of saltating sandgrains. The dimensions of this carpet and the amount of sand that is in motion are determined by the speed of the wind blowing over the surface and the properties of the atmosphere.

The wind over saltating sand. When Bagnold first tried to analyze this process, he found himself in new territory: He corresponded with Prandtl, the foremost expert of his time, but Prandtl's theories apply to pure fluids and need modification before they can be applied to a carpet of saltating sand. Bagnold, thus, developed a rough-and-ready series of estimates that have mostly stood the test of time and are still used to estimate rates of sand transport, with a few minor modifications. He supposed that the wind velocity over a saltating sand carpet is given by:

$$v = 5.75 v'_* \log \left(\frac{z}{z'_0} \right) + v_t \quad (9.12)$$

where v'_* is the friction velocity when sand is in motion. It reflects the increased drag over the flowing sand carpet and is, therefore, larger than the friction velocity when sand is not in motion. The factor z'_0 is a modified roughness, now known as the "aerodynamic roughness," whose nature puzzled Bagnold. Empirically it is about ten times larger than z_0 and Bagnold suggested that it might correspond to the height of ripples. Similarly, v_t is a threshold velocity at height z'_0 . These last two factors must be viewed as empirical fitting factors of obscure physical interpretation. More modern estimates are equally empirical (Greeley and Iversen, 1985). Most recently, however, substantial progress has been made in computing this wind profile using numerical computer codes (Kok and Renno, 2009a).

The flux of wind-driven sand. Bagnold's analysis of the effect of the saltation carpet on the wind near the ground begins with the hop of a single grain. Referring back to Figure 9.2a, a saltating grain first leaps out of the surface and, as it reaches the crest of its trajectory, it is accelerated by the wind to an average horizontal speed u_s . It returns to the bed at its terminal velocity v , so that the angle β at which the saltating grain approaches the bed is given by $\tan \beta = v/u_s$. Each sand grain of mass m thus leaps out of the bed, accelerates from near-zero velocity to final velocity u_s , and then re-impacts the bed a distance l

downwind. This start-stop motion of each saltating grain removes momentum $m u_s/l$ per unit distance from the wind. If the net motion of the sand, comprising many sand grains, is expressed as a mass flux, q_s , per unit width perpendicular to the wind (kg/s-m), this momentum loss per second per unit area equals the drag stress τ' required to keep the sand moving,

$$\tau' = \frac{q_s u_s}{l} \equiv \rho v_*'^2 \quad (9.13)$$

where v_*' is the friction velocity in the presence of a carpet of saltating grains. In his wind-tunnel measurements Bagnold found that u_s/l is approximately equal to the vertical ejection velocity, w , divided by g , $u_s/l \approx w/g$. He then supposed that w is proportional to the friction velocity v_*' . These suppositions lead to a useful scaling relation for the saltation hop length l :

$$l \propto \frac{v_*'^2}{g}. \quad (9.14)$$

The hop height h is proportional to the length through the tangent of the descent angle β .

Inserting the relations in the previous paragraph into Equation (9.13), and solving for q_s , we obtain an expression for the mass flux of the sand in terms of the friction velocity over a moving sand carpet:

$$q_s = C \left(\frac{\rho v_*'^3}{g} \right) \quad (9.15)$$

where C is a “constant” that Bagnold found depends on the square root of the grain diameter. There are many modern variants of Equation (9.15) for the sand flux: Greeley and Iversen (1985) list 15 of them. An obvious improvement is to subtract a threshold friction velocity from v_*' , so that this equation does not predict non-zero fluxes for arbitrarily low velocities. Nevertheless, the important feature of this equation is its dependence on the friction velocity cubed, and that is widely agreed to be at least approximately correct.

The “constant” C in Equation (9.15) conceals factors only partially considered by Bagnold. The rate of sand transport depends on the surface over which the sand saltates: It is slower over sand surfaces, where the saltating grains lose most of their momentum at the end of each hop, and much faster over stony surfaces, a factor that is important in the accumulation of sand patches. The rate of transport also depends on the slope of the surface, a factor that plays a role in modern theories of sand dune formation.

The major implication of Equation (9.15) is that the flux of sand is not a linear function of the wind speed, but depends on the speed raised to the third power. The most important sand-driving winds are, thus, not the average winds, but the exceptional winds. Meteorological plots of average winds may thus be very deceptive when the direction of sand transport is of interest. Gentle winds may blow from one direction most of the year,

but a month of strong winds from another direction may completely dominate the orientation of a dune field. Modern analyses of the wind regime among sand dunes reflect this non-linear dependence of sand transport on the cube of the velocity by plotting a quantity known as the vector drift potential on maps of sand dunes (Fryberger, 1979).

Impact creep and reptation. Although most of the mass moved by the wind travels by saltation, the impulse delivered by the impact of saltating grains contributes up to about 25% of the total. As illustrated in Figure 9.2b, multiple impacts by saltating grains can propel pebbles that are otherwise too big to be moved by the wind. Such pebbles may be seen at the bed of the saltating carpet irregularly jerking or rolling downwind. Recently, an additional type of motion has been distinguished (Lancaster, 1995). Called reptation because the path of the sand grains resembles the slithering of a snake, it describes the motion of coarse sand grains on the bed that are splashed out at low velocity by the impacts of fast-saltating grains.

9.2.3 The entrainment of dust

One of the surprising aspects of wind interaction with the surface is the difficulty of entraining fine particles, dust. Once dust is suspended in the air, it may rise high into the atmosphere, travel over intercontinental distances (Pye, 1987), and may even play a major role in the radiation balance of the atmosphere, as it does on Mars. However, as many observers have noted, dust lying on the surface tends to stay on the surface until something, other than the wind, disturbs it.

Anecdotes about the resistance of fine material to erosion by wind or water abound. Mud mounds in Galveston's harbor survived the catastrophic 1900 hurricane unchanged, while seawalls built of meter-sized rocks were carried away. Gilded Age geologist Raphael Pumpelly was astonished to observe roads in China's loess region entrenched tens of meters into the surface (Figure 9.7), gradually excavated as the dust stirred up by traffic was blown away by the wind. Fine Martian dust that settled over the solar panels of the Spirit and Opportunity rovers was expected to eventually terminate the mission, until dust devils or major sandstorms blasted the dust away.

Bagnold attributed the immobility of dust to its small grain size compared to the thickness of the viscous sublayer in turbulent flow. Greeley and Iversen invoke cohesive forces between small grains. Whatever the cause, neither wind nor water can mobilize fine-grained material without the assistance of some disturbing agency.

Where saltating sand advances over dusty surfaces, the impact of the saltating grains on the surface mixes the dust with the air and thus mobilizes dust. Sand grains and saltating mud chips may play this role in raising dust from terrestrial playas. Sandstorms would be relatively innocuous if they were restricted to the thin carpet of saltating sand, but they are frequently accompanied by thick clouds of dust that do much more damage to the lungs of humans and animals.

On Mars, dust devils seem to play an important role in raising dust from the surface. This has been attributed to the unusually high winds that develop near the core of the dust devil and to the mobilization of low-density aggregates (Sullivan *et al.*, 2008). However, another

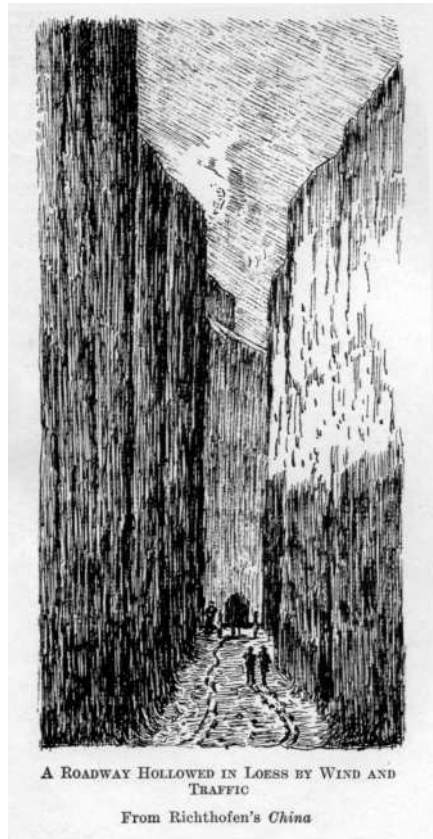


Figure 9.7 A road deeply entrenched in the fine-grained loess terrain in China. This illustrates the fact that fine-grained sediments cannot be moved by the wind until disturbed, in this case by traffic. Once entrained in the air, the wind exports the sediment and the road gradually deepens, with the long-term consequences shown here. Reproduced from Pumpelly (1918, p. 468).

process known as “backventing” or “reverse percolation” may play a role in both dust-devil mobilization and in association with impact-crater blast waves. This process was first proposed in connection with the “dark halos” that were noted in radar images of craters on Venus (Ivanov *et al.*, 1992). It has also been observed in the vicinity of many explosion experiments, but most discussions of it occur in the “gray” literature (Rosenblatt *et al.*, 1982).

Backventing usually accompanies the passage of a shock wave over a dusty surface. In the shock, the pressure first rises above normal atmospheric pressure, then falls below it during the “negative phase” before returning to normal (Glasstone and Dolan, 1977). As the shock wave passes over a permeable surface, it first drives air into the ground, then, during the negative phase, the air vents out of the surface, often carrying dust that has been entrained by direct lofting in the vertical air stream. Optically dark halos up to 1 km in diameter have been noted about the sites of many recent impacts on Mars (Malin *et al.*, 2006) and probably originate by this backventing process. It seems possible that the sudden drop in pressure in the core of a dust devil might also be responsible for initiating a temporary flow of air out of the Martian soil that could entrain and lift dust off the surface, mixing it into the atmosphere.

9.2.4 Abrasion by moving sand

Pebbles and rocks in the path of saltating sand are frequently polished, faceted, and grooved, sometimes leading to fantastic surface patterns. The name ventifact is given to a rock that has been sculptured by the wind. The flux of moving sand is akin to industrial sandblasting and, over time, considerable abrasion of obstacles may occur. R. P. Sharp (1911–2004), in a series of well-known experiments (Sharp, 1964), found that a brick left in the path of saltating sand was half eroded away after 6 yr of exposure. He also planted Lucite rods vertically in the path of the sand and found that the abrasion varied considerably with height: Whereas very little damage occurred above the normal level of the saltating sand, the greatest losses of material were at about 20 cm above the ground, near the top of the saltation layer, while less was removed close to the ground. Hard igneous rocks, on the other hand, suffered little visible damage during the course of his 10.5-year study. Wind abrasion is evidently slow for resistant rocks. Abrasion rates for different materials were quantified in more detail by abrasion experiments conducted in a wind abrasion simulation apparatus by Greeley and Iversen (1985). These experiments showed the widely variable susceptibility of different rock types to wind abrasion at a given impact velocity.

Wind abrasion is a strong function of the impact velocity of individual sand grains, as well as the total flux encountering an obstacle. Because of the lower threshold velocities on Venus and Titan, wind abrasion may not be of great importance there. On Earth, while wind-abraded pebbles adorn the pages of most geology textbooks, they are rare in the field. Wind abrasion is not a widespread process on our planet except in few especially favored locales. However, because of the much higher threshold velocities on Mars, wind abrasion is expected to be more common and, in fact, it did not take long for the Mars Exploration Rovers to encounter wind-fluted rocks (Greeley *et al.*, 2006).

9.3 Eolian landforms

Landscapes dominated by the wind are rare on Earth: Where they do occur they are so strikingly different from our normal experience that they have received a great deal of attention from geomorphologists. While silicate sand or dust is the material most often moved by the wind, blowing snow may also create similar landforms. Mars seems to be the planet most favored by the wind, in spite of its thin atmosphere, although extensive dune fields have also been imaged on Venus and Titan. In the following discussion we will use the term “sand” in its eolian process sense: Sand is loose granular material that moves by saltation.

9.3.1 The instability of sandy surfaces

Much of the interest we find in eolian landscapes derives from their instability. Dune shapes are constantly shifting and dunes are landforms in slow motion. The formation of dunes themselves is due to the instability of surfaces on which sand and larger rocks are mixed.

The flux of saltating sand depends upon the surface across which it moves. Sand grains saltating over sand on Earth leap only a few tens of centimeters off the surface. However, if the sand moves over a stony surface (or a paved road), the grains rebound from the surface with considerably more energy than if they had struck a loose, sandy surface. The saltation height increases dramatically, the high-flying grains sense a faster wind velocity, and the sand moves faster and farther than before. This rapid motion continues until the sand grains reach another sandy patch, where they lose their energy and slow down, many of them dropping out of the wind stream in the process.

A surface of uniformly mixed sand grains and stones thus quickly separates into sandy patches and stony patches as a result of this feedback. This sorting of the surface into sand and stones persists even as the sand accumulates into dune fields, and in spite of the constant downwind migration of the dunes, as Sharp observed in the Algodones Dunes of California (Sharp, 1979).

This tendency for instabilities to grow and create patterns from an initially uniform landscape is presently recognized as a field of study in itself. "Self-organized" pattern formation occurs when positive feedback regulates systems of this kind. Computer models incorporating idealized versions of the laws of sand transport successfully reproduce many features of the natural system, including sand dunes (Anderson, 1996; Werner, 1995). Although such model building is not considered a part of traditional geomorphology, this approach does expose the most important factors that create the observed forms. Pelletier (2008) describes Werner's model, its philosophy, and provides a computer code for implementing it.

9.3.2 Ripples, ridges, and sand shadows

Ripples. The quintessential eolian feature is the sand ripple (Figure 9.8). Wind ripples develop everywhere that loose sand is exposed, on sand dunes, beaches, and even in children's sand boxes. On Earth, they are typically a few centimeters high, spaced about 10 cm apart, and may extend many meters laterally. They are oriented perpendicular to the predominant wind direction and move slowly downwind. Ripples form within minutes in a strong wind. Nevertheless, even after decades of scientific study, their formation still presents many puzzles, the most serious of which have been raised by the observations of what appear to be wind ripples on Mars.

Bagnold noted a similarity between the saltation hop length and the spacing of ripples and concluded that the regular spacing of ripples reflects the average saltation jump length. He supposed that an initially flat sand surface became wavy under the bombardment of the saltating particles, developing so that most saltation hops start and end on the upwind (stoss) side of the ripple, driving intense upslope surface creep, while suppressing creep on the downwind (lee) side

Although Bagnold's identification of saltation length and ripple spacing has been widely accepted, doubts have arisen. Sharp (1963) noted that during windstorms the ripple spacing gradually increases with time, which seems inconsistent with control by the saltation



Figure 9.8 Asymmetric wind ripples in sand. The pocketknife is ca. 10 cm long. Note poorly developed subsidiary ripples at a steep angle to the main trend. Ripples are topped by somewhat coarser sand grains than average. 2000 photo by Jason Barnes, from longitudinal sand dunes near Tuba City, AZ.

length. He proposed instead that the ripple spacing is controlled by the size of the creeping grains and described extensive observations that tend to support his view.

The origin of ripples has currently reached a crisis precipitated by the observations of surface landers and rovers on Mars. By scaling the saltation length from Earth to Mars using Equation (9.14), both the higher threshold friction velocity and lower gravity suggest that a Martian saltation hop should be more than 100 times longer than on Earth, reaching tens of meters or more. If Bagnold's theory is correct, wind ripples on Mars should be spaced tens of meters apart. However, images of the surface show what appear to be Earth-sized "bedforms" everywhere (Mars scientists are reluctant to use the word "ripple" for these features, even though they strongly resemble the terrestrial feature in size and spacing). It seems that, despite the familiar appearance of Martian eolian features, nothing about them fits at the moment. The grain sizes of the material on top of the ridges are too small (200 to 300 μm near the surface, down to 100 μm a few centimeters below the surface), the dust is observed to move when the sand-sized particles do not, and the millimeter-sized particles predicted by the threshold equation (see Table 9.2) are apparently absent (Sullivan *et al.*, 2008), although see Box 9.1 on this topic.

All of these Martian observations suggest that something is seriously amiss in our understanding of what wind processes on Mars are doing. And if our theories are wrong on Mars, are they wrong on Earth as well? New ideas and approaches are urgently needed, such as the suggestion that a very low impact threshold for sand motion on Mars might account for some of the observations (Kok, 2010), or that ripples are actually due to aerodynamic interactions between the wind and roughness elements on the surface (Pelletier, 2009).

Box 9.1 Kamikaze grains on Mars

Wind transport of sand on Mars has long posed a major problem for scientific analysts. Because of Mars' thin atmosphere, the minimum wind velocity required to set particles in motion at the fluid threshold, Equation (9.11) and Table 9.2, is enormous. Note that 69 m/s in Table 9.2 is a wind speed of 250 km/hour one meter above the surface. Do such powerful gales ever blow on Mars? Moreover, the particle size at the threshold of motion is also enormous, of the order of 1 mm, about five times larger than on Earth.

The prospect of a Martian sandstorm is truly fearsome: Anything on the surface would be bombarded by a fusillade of ball-bearing-sized grains flying along at nearly supersonic speeds. Because of this daunting prospect, the cameras of the Viking landers peered out through narrow slits that could be covered in the event of sandstorms. Fortunately, the Viking landers completed their missions before being engulfed in any such destructive sandblasts. But Martian sandstorms must also be highly abrasive to rocks lying on the surface. Indeed, it becomes surprising that there are any intact rocks at all.

Not only would such sandstorms be destructive of hardware on the planet, it should also be destructive of the flying grains themselves. Granting that saltation can get started on Mars, it seems that no sand grain could survive even a single hop before being blasted into dust. Significantly, it seemed, Viking soil-sieve measurements showed a deficit of grain sizes in the millimeter range. This observation has, moreover, been confirmed by the Spirit rover's microscopic imaging system (Sullivan *et al.*, 2008).

This problem became known as the "kamikaze effect": Martian sand grains can hop once, then they die. This begs the question of where sand grains come from in the first place. If this is their fate on Mars, then there cannot be very many of them.

The difficulty of getting sand grains to either move or survive on Mars, coupled with the undoubted observation of sand dunes, led to a variety of proposals for how Mars manages to build sand dunes in spite of its thin atmosphere. So far, no definitive solution has been found. The leading idea is that the sand grains that saltate are not solid particles at all, but instead are aggregates of finer material somehow cemented into millimeter-sized pellets. The lower density of such grains would make entrainment by the wind easier, although it would exacerbate the survival problem. However, even if the grains are destroyed after one hop, their fragments might be re-cemented at a later time to prepare them for another hop. Clay dunes (lunettes) on Earth form in this way, and such dunes, while relatively rare on Earth, have received a lot of attention from the Mars scientific community.

Another possibility is that the Martian sand dunes cannot, in fact, move under current climatic conditions and they are all relicts from a time when Mars' atmospheric pressure was higher. As of this writing, the HiRISE imaging system has not observed any dunes to move, at a resolution of about 30 cm. However, the Spirit rover reported that after strong wind gusts, grains up to 300 μm in diameter appeared on its top deck. While these are smaller than predicted at the fluid threshold, the fact that they were in motion at all is something of a surprise. Because the megaripples investigated by Spirit at El Dorado crater are composed of grains of this size, it seems that at least megaripple-forming materials are mobile during high winds.

Box 9.1 (cont.)

A very new idea, mentioned in Section 9.2.1, is that the fluid threshold might not be relevant on Mars. The impact threshold may occur at a much lower velocity on Mars so that the 100 μm to 300 μm particles that make up the megaripples could be the dominant grain size on Mars. Once they are in motion, grains of this size require much lower velocity winds to sustain them and, at this lower velocity, are not imperiled by impact destruction after one saltation hop.

Our understanding of the humble, ubiquitous ripple is certainly in need of improvement. One of the main drivers in this urgent need is the crisis raised by observations made on another planet than the Earth, highlighting the importance of comparative planetology even for those interested only in the Earth.

Ridges. Bagnold also noted that many large ripples (he called them “giant sand ridges”) had coarser grains at their crests and suggested that surface creep of the larger grains drove them to the crest and then armored the crest sand against further deflation. Many subsequent observations of sandy ridges that are bigger than ripples but smaller than dunes have agreed with his observation that their grain size distributions are typically bimodal, and that the coarse grains collect at the crest of the ridge. These ridges are long-lasting and, like ripples, form transverse to the prevailing wind.

Some of the puzzling Martian eolian ridges may be of similar origin: The Spirit rover has confirmed the bimodal distribution of grain sizes in several ridges in Gusev crater. These features should, thus, properly be considered ridges, not large ripples, in spite of the unfortunate terminology: “Megaripples” lie everywhere on Mars. Megaripples form transverse to the wind and range from tens of centimeters up to 3 m high and a few to tens of meters apart (Figure 9.9). Many are light-colored, in contrast to the mainly dark dunes of basaltic sand and may be composed of a different material, perhaps low-density dust aggregates.

Sand shadows. Actively moving sand requires wind to keep it in motion. When the wind strength drops, sand accumulates. This simple fact accounts for the accumulations of sand commonly found in the lee of large rocks, brush, and in hollows below the general level of the surface. On Mars, this accounts for the wind-blown material in the lee of crater rims and in their interiors. Small dune fields typically form in the interiors of Martian craters where sand has accumulated and the wind speed is reduced.

Ripples often curve sharply when they cross sand shadows, their curvature indicating the deflection of the surface wind by the obstacle: The wind direction is always perpendicular to the trend of the ripples. One may, thus, note the divergence of the wind upwind of the obstacle and its convergence behind. The antitheses of shadows, sand scours, often develop upwind of obstacles where the wind speed accelerates.

A characteristic pattern of sand shadows and scours develops around small craters, illustrated in Figure 9.10. These organized zones of deposition and scouring are the result of twin eddies shed downwind as the wind parts around the crater rim. Sand accumulations

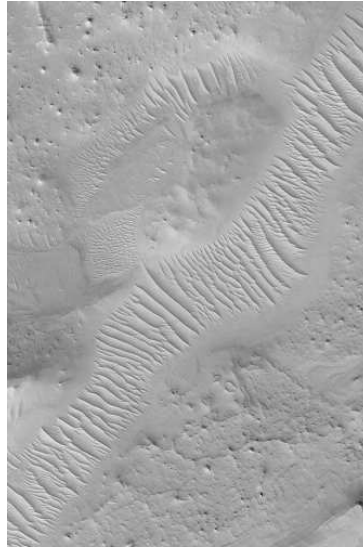


Figure 9.9 Megaripples on Mars. Ripples lie on the floor of a channel at 29.34° N and 299.83° W. Image is 3 km wide. Upper portion of Mars Orbiter Camera (MOC) image 1200991.

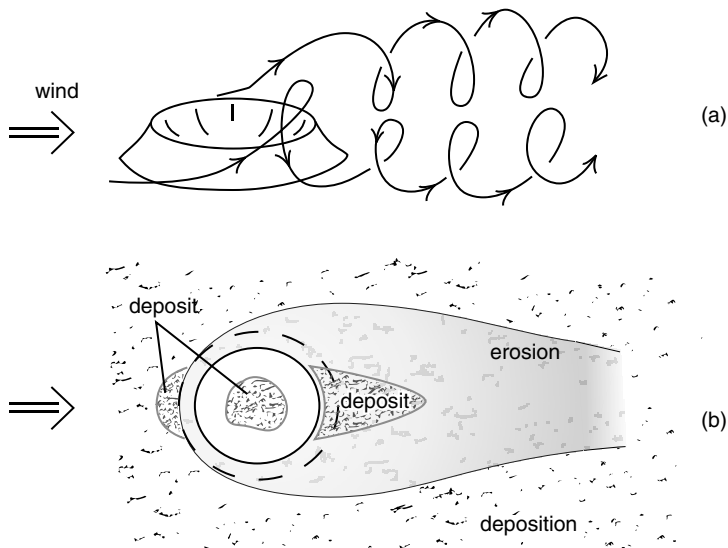


Figure 9.10 Sand shadows behind Martian crater forms. As the wind blows, vortices form and detach from the upwind rim of the crater. Sand is deposited in less windy areas upwind of the crater, in its interior, and immediately downwind of the rim, while the increased wind velocity in the vortices leads to enhanced erosion along the sides and farther downwind of the crater. Interpretation inspired by illustrations in Chapter 6 of Greeley and Iversen (1985).

behind mountain ridges are called “falling dunes,” but frequently are merely immobile sand that has collected in the lee of the ridge.

9.3.3 Dunes

Sand dunes are larger accumulations of sand that are too wide for saltating grains to hop across. As dunes grow higher they create zones of quiet air or even reversed flow in their lee and, thus, block the saltation flow across the surface. Such shadow zones lead to the accumulation of more sand behind the crest, building the dune higher until the slope of the lee face reaches the angle of repose. At this point a “slip face” develops where sand that has arrived at the crest avalanches down the face.

Dunes are self-organized forms that grow spontaneously when conditions are right. They may start simply as a patch of sand on a stony plain that tends to capture more sand, which leads to the capture of still more sand in a strong positive feedback. Sand dunes would grow to unlimited height if given an unlimited supply of sand, except that as they grow they deflect the wind over their tops, increasing its velocity and eventually blowing sand off their crests faster than it can continue to build upward.

Dune velocity. All the time that a sand dune is growing in volume it is also moving downwind. The speed of downwind motion is easy to calculate and the result is very instructive. If q_s is the mass rate of sand movement per unit distance perpendicular to the wind, the rate at which it adds volume to the lee side of the sand dune (Figure 9.11) is q_s/σ_s , where σ_s is the density of loose sand in the dune. In each interval of time Δt the sand blown over the brink fills a prism in the lee of the dune of height h , length Δx and volume $h \Delta x$. The volume of this prism is equal to the volume of the sand blown in, $q_s \Delta t / \sigma_s$, so the dune creeps downwind at a velocity:

$$v_D = \frac{\Delta x}{\Delta t} = \frac{q_s}{\sigma_s h}. \quad (9.16)$$

Naturally, the dune velocity increases as the rate of sand transport increases. The interesting thing about this equation is that the velocity depends *inversely* on the dune height. This does make a lot of sense: It takes more sand to build a taller dune one unit of distance downwind than it does for a smaller dune. However, this means that the taller a dune grows, the slower it moves.

In a dune field in which a number of both large and small dunes occur, the small dunes race along while the big dunes lumber downwind. But when a small dune overtakes a big one, it climbs up its upwind face and collapses down the slip face, feeding the big dune while it is itself annihilated. The big dunes, thus, tend to grow at the expense of the small ones, looming larger and slower until the accelerated winds at their tops blow sand off their summits as fast as it accumulates and they reach a fixed height. Even this, however, does not stop their inexorable movement – they continue to crawl downwind until some new fate consumes their sand.

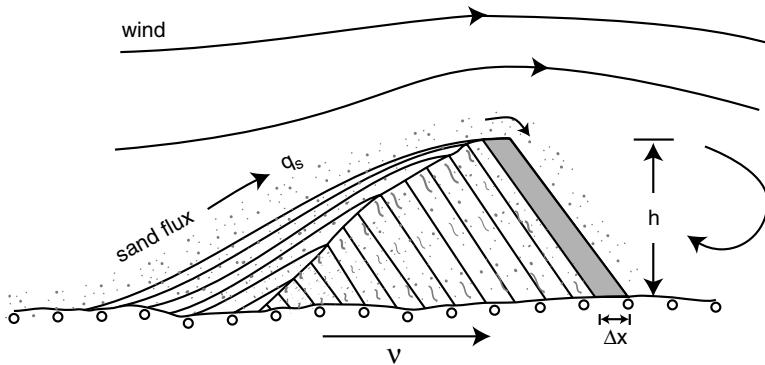


Figure 9.11 Downwind migration of sand dunes. The migration velocity of a sand dune is computed by balancing the sand flux moving up the upwind face of the dune against the volume required to build the dune one unit of length downwind. Sand is immobilized in the lee of the dune after it moves over the crest, where it accumulates at the angle of repose.

An important concept for interpreting the formation of dunes is the timescale over which an individual dune forms (Allen, 1974). In a regime of changing climate, large dunes may reflect conditions from a different climatic era and their morphology may thus be out of harmony with the regime prevailing at the time they are observed. A useful timescale is derived by comparing the volume of a dune with its rate of growth or, equivalently, the length of time required for the dune to move its own length,

$$\tau_D = \frac{\lambda h}{v_D} = \lambda h^2 \frac{\sigma_s}{q_s} \quad (9.17)$$

where λ is the length/height ratio of the dune, typically equal to about 10. This “dune modification timescale” on Earth ranges from a few years for small dunes to 50 000 yr for large star dunes.

Dunes and dune fields are classified in various ways, but a common division groups them by their orientation with respect to the predominant wind. Dunes are, thus, considered to belong among the transverse, longitudinal, or star classes, depending on whether they are oriented perpendicular to the prevailing wind, parallel to it, or are heaped chaotically with no particular direction evident. There are special classes of dune, such as parabolic dunes, that are dependent upon vegetation to create their form. In this book such forms are ignored, but they are very important in terrestrial geology, particularly along coasts where vegetation is common. In addition to the “pure” forms described below, compounds of different types are almost universal.

Barchan dunes. The classic dune type is the barchan (Figure 9.12a). Shaped like a crescent lying with its convex side upwind, barchan dunes form spontaneously on stony plains where sand is in short supply. Barchans on both the Earth and Mars grow to an approximately constant size in a given area and maintain their characteristic shape as they migrate downwind. On Earth, barchans range from about 3 to 10 m in height and extend about 30

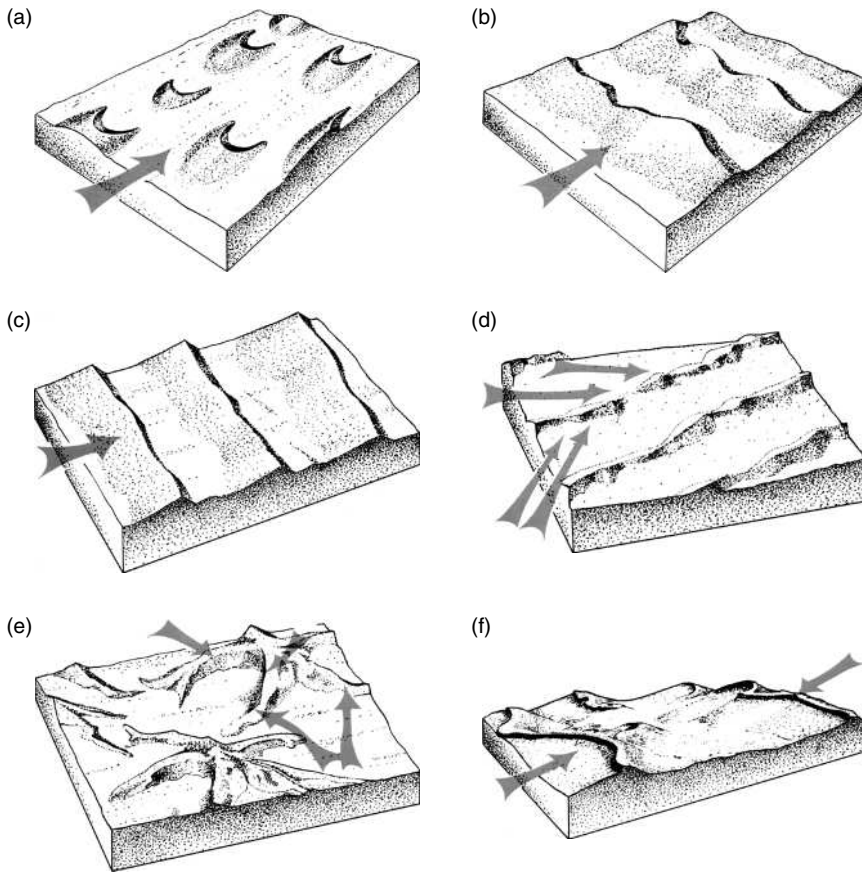


Figure 9.12 Different dune patterns are determined by both the wind regime and sand supply. (a) Barchan dunes form where a unidirectional wind drives a limited supply of sand. (b) Barchanoid ridges with wavy crests form transverse to the wind when more sand is available. (c) Full transverse dunes develop where sand is abundant and the wind is unidirectional. (d) Linear or longitudinal dunes form where the wind blows from more than one direction, but are generally parallel to the dominant wind direction. (e) Star dunes form under conditions of multiple wind directions with none dominant. (f) Reversing dunes are created by unidirectional winds that occasionally reverse themselves. All images from McKee (1979, pp. 11, 13).

to 100 m downwind. Their upwind slopes are gentle, standing at angles of about 5° to 15° , while the slip face stands at the angle of repose, near 32° . Surprisingly, barchan dunes on Mars are about the same size, despite the difference in surface conditions. The upwind face of barchan dunes is symmetrically arched in plan view, while an arcuate slip face develops downwind and lateral horns grade into low mounds lacking slip faces. Because the slip face traps migrating sand and thus prevents it from moving further downwind, barchans shed sand only off their lateral horns. The barchan form seems remarkably stable and these dunes are capable of migrating large distances downwind without change of form.

As the sand supply increases, instead of increasing in size indefinitely, barchan dunes shed sand off their horns, which may then organize itself into small new barchans, a reproductive process that fascinated Bagnold, who described it in the introduction to his book as “vaguely disturbing” in its “grotesque imitation of life.”

Barchan dunes are most symmetrical when the wind blows from a single direction. When lateral winds occur, one horn grows larger and longer than the other, with the larger horn developing on the upwind side with respect to the lateral wind direction. With persistent lateral winds barchans may grade into linear dune chains.

Transverse dunes. With increasing sand supply and a constant wind direction, isolated barchan dunes merge into long ridges oriented perpendicular to the wind. Such ridges stretch many kilometers laterally and are repeated downwind by parallel ridges, creating a landscape dominated by parallel ridges with undulating crests. When the crests of these ridges are sinuous in plan they are often called “barchanoid” ridges (Figure 9.12b), but are simply called “transverse dunes” when their crests are more linear (Figure 9.12c). On Earth, there is a crude relation between the height and spacing of these dunes: Dunes a few meters high are spaced about 100 m apart, while dunes 100 m tall are spaced about 1 km apart (Lancaster, 1995).

The regular spacing of transverse dunes is likely due to aerodynamic flow patterns: The presence of a ridge suppresses surface winds for some distance downwind. Such shadow zones extend 12 to 15 times the height of the obstacle, in agreement with the observed spacing. Reverse eddies may also develop between the ridges, and many observers have noted weak winds blowing up the slip face of tall dunes while sand was blowing downwind over the crest.

All of the dune fields imaged on Venus belong to the transverse type, as indicated by their perpendicular orientation to wind streaks (Greeley *et al.*, 1997). Magellan could only resolve the largest dunes, which seem to be spaced about 0.5 km apart with ridges trending 5 to 10 km perpendicular to the wind direction. Magellan could not measure the heights of the dunes.

The transverse dune type also dominates on Mars, although large areas are occupied by sparsely scattered barchan dunes (Greeley *et al.*, 1992). Martian transverse dune ridges are typically spaced 300 to 800 m apart. Most of the large dune fields lie in the northern circumpolar plains. Two varieties of transverse dune are observed in small clusters, mostly lying within craters. The smaller variety is spaced 100–1200 m apart, while the larger variety is spaced at 1600–4000 m. Martian dunes are typically dark and are believed to be composed mostly of basaltic sand.

Linear dunes. Impressively long, linear dunes traverse large areas of the Earth and Titan (Figure 9.13). On Earth, individual linear dunes range from about 20 km to 200 km long, 2–35 m high and are spaced about 200–450 m apart. Compound versions of these dunes may be much larger: 50–170 m high and spaced 1600–2800 m apart. Dunes on Titan cover a vast area of the satellite, occupying about 40% of the low-latitude half of Titan, a larger fractional surface coverage than on any other body in our Solar System (Jaumann *et al.*, 2009). Titan’s dunes are estimated to be about 30–70 m high with an average spacing of 2

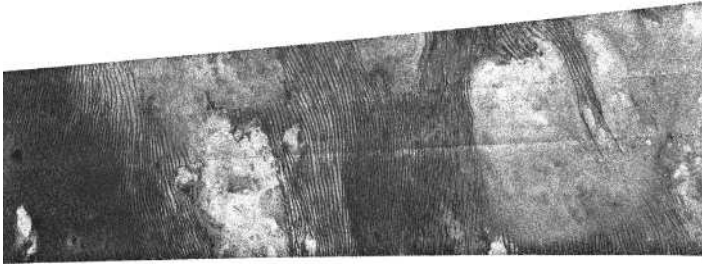


Figure 9.13 Longitudinal dunes in the equatorial region of Titan, which likely consist of sand-sized particles made of organic material. Notice that the dunes are deflected by the brighter (and presumably higher) terrain, following the wind direction. The imaged area is 225 x 636 km from the T-25 pass of the Cassini orbiter Synthetic Aperture Radar. North is to the right. PIA12037: NASA/JPL.

km. Chains of dunes can be traced hundreds of kilometers. The dominance of linear dunes on Titan may be connected with its unique wind regime, in which the surface winds are mainly driven by tides rather than thermal gradients.

Linear dunes, called seif dunes by Bagnold, form when the sand-moving winds blow from more than one direction (Figure 9.12d). One direction must predominate, which determines the trend of the dunes, but they require a crosswind from another direction for at least part of the year. Because of this inconstant wind regime, the crests of linear dunes are often irregular and small slip faces alternate from one side to another.

The impressively parallel trend and spacing of linear dunes may be maintained by the formation of alternate helical eddies aligned with the prevailing wind. This idea was first proposed by Bagnold and has been popular with many subsequent authors. However, direct measurements of the sizes of helical eddies often do not agree with the observed dune spacing. At the moment, there is no universally agreed process that controls the lateral spacing of linear dunes.

Star dunes. Where no predominant wind direction exists, the direction of sand transport shifts constantly and sand piles up into huge, complex heaps known as star dunes. Strictly speaking, a star dune must have at least three arms containing slip faces (Figure 9.12e). The tallest accumulations of sand on Earth are star dunes, with heights that reach up to 4 km, but are more typically a few hundred meters high. Star dunes are spaced at distances equal to about ten times their height, a common dimensional ratio among dunes.

Reversing dunes. In areas where the wind regularly reverses direction, slip face directions may alternate from one side of a dune to another. Strictly speaking, reversing features occur at the crest of larger accumulations of sand: Because the reversal timescale is short, the volume of the reversing portion of a dune cannot be large. Nevertheless, the crests of reversing dunes are distinctively symmetrical, with triangular profiles (Figure 9.12f). Barchan dunes will also tolerate an exact reversal of the wind direction without major effects on their morphology, so long as one direction predominates.

Many other dune forms and features have been identified and named. Lunettes, for example, develop around the downwind margins of playa lakes and are often composed

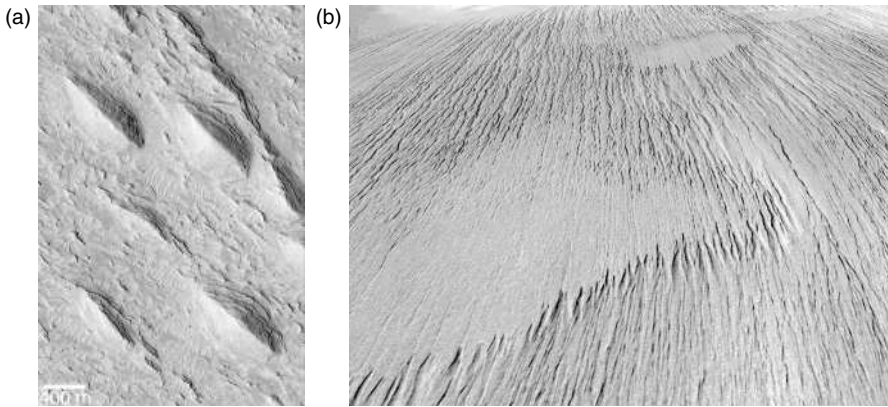


Figure 9.14 Yardangs on Mars. (a) Closeup view of yardangs showing the classic “inverted boat hull” morphology, located near 1° N, 214.4° W. Scale bar at the lower left is 400 m. MOC image PIA04677 NASA/JPL/Malin Space Science Systems. (b) Panoramic view of a soft rock unit dissected into yardangs south of Olympus Mons. The three flat regions in the fore-, middle-, and background measure about 17 x 9 km in this oblique view. Mars Express HRSC image, orbit 143, ESA/DLR/FU Berlin. (G. Neukum). See also color plate section.

of fine-grained material, even clay, whose particles are normally too small to saltate as individuals. However, when cemented by salts or after wetting, these fine particles become weakly cemented into aggregates that can be moved short distances by the wind.

Climbing dunes, as opposed to falling dunes, are special forms that develop on steep slopes upwind of resistant ridges over which the sand eventually passes, to accumulate into falling dunes on the lee side. For more detail on the range of types recognized, the reader is referred to the specialized literature, such as the book by Lancaster (1995).

9.3.4 Yardangs and deflation

Dunes are depositional landforms in which material accumulates. Yardangs are the characteristic erosional form created by the wind (Blackwelder, 1934). On Earth, yardangs are a minor geomorphic curiosity, seldom seen by anyone but travelers in arid regions. Where they occur, they are usually small, only fractions of a meter to at most tens of meters high and up to 20 m apart. They usually develop in weakly cohesive rocks such as clay, silt, or weakly cemented sandstones. Yardangs appear as long, linear ridges with streamlined upwind edges whose shape many observers have compared to overturned boat hulls (Figure 9.14a). Saltating sand erodes the troughs between yardangs only along their floors, so the ridges are often undercut along their sides and upwind edges. The troughs are typically flat-floored or U-shaped.

Whereas yardangs are only minor features on Earth, they dominate some landscapes Mars (Figure 9.14b). Weak, perhaps pyroclastic, rock layers near the Martian equator are deeply entrenched by linear grooves aligned with the prevailing wind. The edges of mesas

are often deeply etched by yardangs and crater ejecta deposits are dissected into linear ridges. Yardangs on Mars are enormous by terrestrial standards, tens of kilometers long and separated by troughs averaging 200 m wide.

Yardangs may also be extensive on Venus. Although difficult to identify unambiguously from Magellan radar images, Greeley *et al.* (1997) described an extensive field of yardangs about 500 km southeast of Mead crater. These yardangs, if that is what they are, average 25 km long by 0.5 km wide and are spaced from 0.5 to 2 km apart.

Dust-raising winds may also erode shallow, closed depressions, in strong contrast to fluvial processes, which tend to fill in closed basins. Called deflation hollows or pans on Earth, such depressions range from “buffalo wallows” only a few tens of meters across to the Qattara Depression in Egypt, a shallow, crescent-shaped basin more than 100 km wide and 200 km long that has been excavated 134 m below sea level. The Qattara Depression may have formed as recently as the past 2 Myr, suggesting a very high rate of eolian erosion, even by terrestrial standards. Deflation hollows have not yet been definitively identified on other planets, perhaps due to the difficulty of ruling out other processes that create shallow depressions. Any persistent source of eolian dust must eventually evolve into a shallow basin of this kind.

9.3.5 Wind streaks

Images of wind streaks returned by the Mariner 9 orbiter provided the first evidence for wind action on Mars (aside from the global dust storms themselves). Seen as variable albedo patterns in the lee of obstacles such as crater rims, Martian wind streaks puzzled early observers: some were bright and some were dark. Sometimes both bright and dark streaks formed around the same feature (Figure 9.15). Martian wind streaks change with time: They are especially likely to have changed after dust storms. We now believe that most Martian sand materials are dark, of mainly basaltic composition, whereas the ubiquitous red or orange dust is bright, a simple fact that resolves many puzzles involving albedo markings on Mars.

Wind streaks have no topographic expression. They result from the deposition or removal of thin deposits of wind-blown material whose color or brightness contrasts with the underlying surface. They are common on Earth as well as Mars. They appear often in snow-covered terrains, but more permanent streaks have formed behind obstacles such as cinder cones. The well-studied wind streak downwind of Amboy Crater in southern California is a good example that can be readily seen in Google Earth images. This particular streak is more permanent and appears to result from differential trapping of light-colored sand on dark desert pavements near the cinder cone.

Both bright and dark wind streaks were observed downwind of Venusian craters by Magellan’s radar. In radar images, “bright” means “rough” (at the radar wavelength, 12.6 cm) and may, in this case, imply removal of fines by enhanced turbulence downwind of the crater. Dark streaks imply deposition of smooth material. Analysis of Magellan images revealed almost 6000 wind streaks (Greeley *et al.*, 1997) that were used to map global atmospheric circulation patterns.

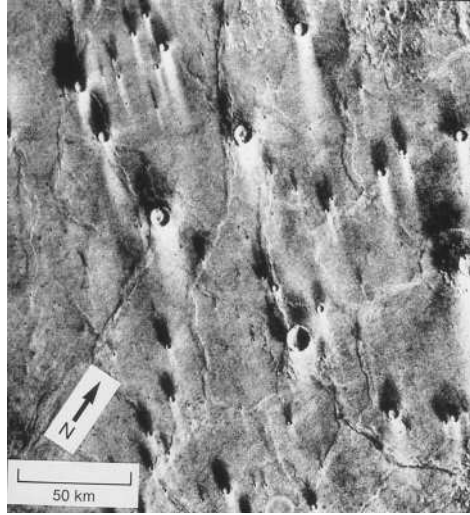


Figure 9.15 Bright and dark wind streaks are simultaneously present around craters on Mars. These presumably formed during different wind regimes and are the result of the differential vulnerability of dark basaltic sand and bright dust to wind erosion or deposition. Image is located at 28° S, 245° W in Hesperia Planum. Viking Orbiter frame 553A54. NASA/JPL.

9.3.6 *Transient phenomena*

Patterns resulting from eolian deposition can often be observed on the surfaces of planets. Global dust storms on Mars redistribute dust on an almost annual basis, obscuring areas previously cleared of dust by impact blast waves or dust devils. Dust-devil tracks a few tens of meters wide and many kilometers long criss-cross dusty plains, appearing dark after the removal of the bright dust.

Volcanic eruptions create plumes of airborne volcanic dust that settles out downwind for distances that may reach thousands of kilometers on Earth. Close to the volcano where deposits of volcanic tephra are thick, winds may heap the fine material into dunes.

The ejecta from impact craters also interact with the atmosphere to create deposits similar to those of volcanoes, although organized somewhat differently. Notable impact-related features are the dark crater parabolas on Venus (Figure 9.16). Radar-dark, parabola-shaped features surround about 60 fresh Venusian craters. With blunt ends facing almost due east, parabolas stretch a few hundred to more than 2000 km from east to west and extend up to 1000 km from north to south at their widest extremities. These features are successfully explained as the fine-grained ejecta deposits of impact craters (Schaller and Melosh, 1998; Vervack and Melosh, 1992). Although the impact throws out ejecta basically symmetrically, most of the distal ejecta fall back into the atmosphere after a short ballistic flight. After re-entry it drifts with the wind as it settles toward the surface. The upper atmosphere of Venus flows steadily from east to west at speeds up to 60 m/s at 50 km altitude. The ejecta drifts downwind, traveling westward as it settles. Because the ejecta falling closer to the

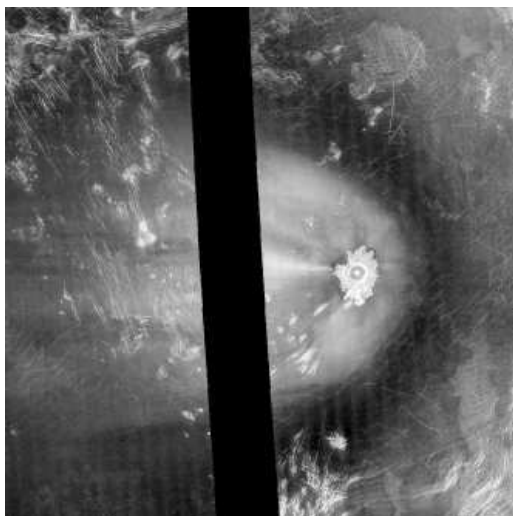


Figure 9.16 Adivar Crater on Venus and its parabolic ejecta deposits. Adivar is 30 km in diameter, located at 9° N, 76° E, and is surrounded by an inner radar-bright (rough) parabola, which is in turn surrounded by a radar-dark (smooth) parabola. This image is 674×674 km, showing the enormous extent of these deposits, which probably represent coarse ejecta close to the crater and finer material that fell back into the atmosphere farther away and was blown westward by strong prevailing winds in the upper atmosphere. Portion of Magellan Radar Image C2-MIDR.00N080;1. NASA/JPL.

crater is coarser than that falling farther away, the closest ejecta is deposited first, while the more distal ejecta blows farther downwind, creating the parabolic shape. The details of the parabolas' shapes even permits the particle size to be inferred and yields a general relation between ejecta particle size, ejection velocity, and crater size for large impact craters. This information could probably not be gained in any other way, short of arranging for a series of large impacts.

Further reading

The fundamentals of the transport of sand and dust by wind are well treated by, obviously, Bagnold (1941) as well as in a later USGS report (Bagnold, 1966). A more modern treatment from the planetary perspective can be found in Greeley and Iversen (1985). Dust deposition and transport is the subject of Pye (1987), while the standard work (which includes many spectacular images) is McKee (1979). A more modern treatment of dunes is given by Lancaster (1995). Wind erosion and deposition by wind on the Earth is well described in an older classic (Mabbutt, 1977). The “planetary connection” is made by a series of long papers: For Venus, see Greeley *et al.* (1997); for Mars see Carr (2006). Our knowledge of Titan is relatively recent, but a good summary of what we do know is in Jaumann *et al.* (2009).

Exercises

9.1 *The looming clouds?*

Clouds on Earth are composed of water droplets whose density, about 1000 kg/m^3 , is much larger than the density of air (about 1.3 kg/m^3 at the surface of the Earth). So why don't the clouds simply fall out of the sky? Discuss this problem in the light of Stokes' law for the rate of fall of small particles. You may find it useful to know that the average size of cloud droplets is about $10 \text{ }\mu\text{m}$.

9.2 *Blowing in the wind or falling like a brick?*

Small meteorites (weighing a few milligrams) that enter the Earth's atmosphere typically evaporate at altitudes near 70 km as they flare up briefly as "shooting stars." The refractory silicates that compose most of these small meteorites then condense into "smoke" particles with sizes that range from 1 to 3 nm . An estimated total of about 100 tons/day of such material currently falls into the Earth's atmosphere. Estimate how long particles of this size might stay aloft in the atmosphere. Compare this to the time that a large, solid, meteorite fragment, 20 cm in diameter, takes to fall to the surface.

9.3 *Do the math!*

Derive Equation (9.9) in the text for the threshold velocity of the wind to just move a sand grain of diameter d lying on the surface.

9.4 *Sand dunes on Triton?*

Triton, Neptune's largest moon, possesses a very thin atmosphere that is composed mainly of N_2 gas at a chilly 38 K . Nevertheless, geysers spout plumes 8 km high into the atmosphere. Suppose that loose "sand" grains of ice (perhaps from impact ejecta) lie on the surface. How fast do the winds of Triton have to blow to just entrain such ice grains, and how big are these grains? Compute both the minimum friction velocity needed to loft these grains and the minimum wind speed 1 m above the surface. Compare this velocity to the speed of sound in Triton's atmosphere. What can you conclude about the probability of finding "sand" dunes on Triton if it is visited by a spacecraft with an imaging system capable of resolving such features? Facts that you may find useful: The viscosity of nitrogen gas at 38 K is about $2.2 \times 10^{-6} \text{ Pa}\cdot\text{s}$ and its density at Triton's atmospheric pressure of 1.5 Pa is $1.3 \times 10^{-4} \text{ kg/m}^3$. The acceleration of gravity at the surface of Triton is 0.78 m/s^2 .

9.5 *The marching dunes*

The Algodones Dunes along the eastern margin of southern California's Imperial Valley exhibit slip faces up to 40 m high. Large complex transverse dunes alternate with interdune

flats that are typically about 500 m to 1 km wide. The dunes themselves are about the same width as the interdune flats. R. P. Sharp (1979) measured the rate of the downwind migration of these dunes to be about 35 to 40 cm/yr. From this data estimate the average sand flux along the dune chain and the lifetime of an individual dune in the field. The California Department of Transportation is contemplating the construction of a new highway about 50 m downwind of a small outlier dune with a slip face 5 m high. Discuss the wisdom of this plan.